NASA/TM—2012-217446 AIAA–2012–1033

Exhaust Plume Effects on Sonic Boom for a Delta Wing and a Swept Wing-Body Model

Raymond Castner
Glenn Research Center, Cleveland, Ohio

Troy Lake
Wichita State University, Wichita, Kansas

April 2012

NASA STI Program . . . in Profile

Since its founding, NASA has been dedicated to the advancement of aeronautics and space science. The NASA Scientific and Technical Information (STI) program plays a key part in helping NASA maintain this important role.

The NASA STI Program operates under the auspices of the Agency Chief Information Officer. It collects, organizes, provides for archiving, and disseminates NASA's STI. The NASA STI program provides access to the NASA Aeronautics and Space Database and its public interface, the NASA Technical Reports Server, thus providing one of the largest collections of aeronautical and space science STI in the world. Results are published in both non-NASA channels and by NASA in the NASA STI Report Series, which includes the following report types:

- TECHNICAL PUBLICATION. Reports of completed research or a major significant phase of research that present the results of NASA programs and include extensive data or theoretical analysis. Includes compilations of significant scientific and technical data and information deemed to be of continuing reference value. NASA counterpart of peer-reviewed formal professional papers but has less stringent limitations on manuscript length and extent of graphic presentations.

- TECHNICAL MEMORANDUM. Scientific and technical findings that are preliminary or of specialized interest, e.g., quick release reports, working papers, and bibliographies that contain minimal annotation. Does not contain extensive analysis.

- CONTRACTOR REPORT. Scientific and technical findings by NASA-sponsored contractors and grantees.

- CONFERENCE PUBLICATION. Collected papers from scientific and technical conferences, symposia, seminars, or other meetings sponsored or cosponsored by NASA.

- SPECIAL PUBLICATION. Scientific, technical, or historical information from NASA programs, projects, and missions, often concerned with subjects having substantial public interest.

- TECHNICAL TRANSLATION. English-language translations of foreign scientific and technical material pertinent to NASA's mission.

Specialized services also include creating custom thesauri, building customized databases, organizing and publishing research results.

For more information about the NASA STI program, see the following:

- Access the NASA STI program home page at *http://www.sti.nasa.gov*

- E-mail your question via the Internet to *help@sti.nasa.gov*

- Fax your question to the NASA STI Help Desk at 443–757–5803

- Telephone the NASA STI Help Desk at 443–757–5802

- Write to:
  NASA Center for AeroSpace Information (CASI)
  7115 Standard Drive
  Hanover, MD 21076–1320

NASA/TM—2012-217446 AIAA–2012–1033

Exhaust Plume Effects on Sonic Boom for a Delta Wing and a Swept Wing-Body Model

Raymond Castner
Glenn Research Center, Cleveland, Ohio

Troy Lake
Wichita State University, Wichita, Kansas

Prepared for the
50th Aerospace Science Conference
sponsored by the American Institute of Aeronautics and Astronautics
Nashville, Tennessee, January 9–12, 2012

National Aeronautics and
Space Administration

Glenn Research Center
Cleveland, Ohio 44135

April 2012

This work was sponsored by the Fundamental Aeronautics Program at the NASA Glenn Research Center.

Level of Review: This material has been technically reviewed by technical management.

Available from

NASA Center for Aerospace Information
7115 Standard Drive
Hanover, MD 21076–1320

National Technical Information Service
5301 Shawnee Road
Alexandria, VA 22312

Available electronically at http://www.sti.nasa.gov

Exhaust Plume Effects on Sonic Boom for a Delta Wing and a Swept Wing-Body Model

Raymond Castner
National Aeronautics and Space Administration
Glenn Research Center
Cleveland, Ohio 44135

Troy Lake
Wichita State University
Wichita, Kansas 67260

Abstract

Supersonic travel is not allowed over populated areas due to the disturbance caused by the sonic boom. Research has been performed on sonic boom reduction and has included the contribution of the exhaust nozzle plume. Plume effect on sonic boom has progressed from the study of isolated nozzles to a study with four exhaust plumes integrated with a wing-body vehicle. This report provides a baseline analysis of the generic wing-body vehicle to demonstrate the effect of the nozzle exhaust on the near-field pressure profile. Reductions occurred in the peak-to-peak magnitude of the pressure profile for a swept wing-body vehicle. The exhaust plumes also had a favorable effect as the nozzles were moved outward along the wing-span.

Nomenclature

AOA	Angle of attack, degrees
B	Nozzle boat-tail angle, degrees
c	Airfoil chord, in.
D	Nozzle diameter (outer), in.
h	Distance below vehicle, in.
L_v	Vehicle length, in.
M_∞	Free-stream Mach number
NPR	Nozzle pressure ratio = P_t / P_∞
P	Local static pressure, psia
P_t	Total pressure in nozzle, psia
P_∞	Free-stream static pressure, psia
ΔP	$P - P_\infty$
$\Delta P/P$	$(P - P_\infty)/ P_\infty$
T_o	Nozzle total temperature, R
T_∞	Free-stream total temperature, R
t	Airfoil thickness, in.
x	Distance along abscissa of pressure signature, in.
y	Distance from nozzle centerline, in.

1.0 Introduction

Supersonic travel is not allowed over populated areas due to the disturbance caused by the sonic boom. At the vehicle nose there is a rise in pressure, followed by a steady decrease to negative pressure, followed by a rise to atmospheric pressure. When propagated to the ground, this pressure profile takes the shape of an N-wave. The two large pressure changes create a "double boom" effect. The impact of the sonic boom is so large that the FAA has issued a noise policy for supersonic aircraft stating: "Since March 1973, supersonic flight over land by civil aircraft has been prohibited by regulation in the United States. The Concorde (Ref. 1) was the only civil supersonic airplane that offered service to the United States, and it is no longer in service" (Ref. 2). The same policy also states that "noise operating rules would propose that any future supersonic airplane produce no greater noise impact on a community than a subsonic airplane." Subsonic noise limits are prescribed in 14 CFR Part 36 stage 4.

To create an aircraft with acceptable noise, programs such as the Quiet Spike (Ref. 3) and the Shaped Sonic Boom Demonstrator (SSBD) (Ref. 4) reduced the intensity of the nose shock wave. Most research has been focused on reducing the sonic boom contribution caused at the front of the vehicle, and less research has occurred in reducing the contribution from aft structures or nozzle exhaust. One exception, Putnam (Ref. 5), performed a study of exhaust nozzles and the effects of the exhaust plume. Tests were done in the 4- by 4-Foot Supersonic Wind Tunnel with pressure measurements taken one diameter away from the nozzle.

Exhaust nozzle plume effect on sonic boom has progressed from analysis and testing of an isolated nozzle (Refs. 6 and 7), to analysis of a slot nozzle embedded in a simplified wing geometry (Ref. 8), to analysis of a single engine wing-body model (Ref. 9), to the present analysis of a multi engine wing-body model. For the isolated nozzle, it was shown how the lip shock from an under-expanded nozzle plume could suppress the nozzle boat-tail expansion and reduce the trailing shock. Similar results were found for the slot nozzle embedded in the wing, where the trailing shock caused by the wing expansion was reduced by the addition of an under-expanded nozzle plume. Results for a single engine wing-body model also demonstrated a reduction in the trailing shock by including an under-expanded nozzle plume.

The subject of this report is the preliminary study of a simplified wing-body configuration with the addition of four engine exhaust nozzle plumes. The purpose is to provide a baseline analysis of a generic wing-body configuration, and demonstrate the effect of the nozzle exhaust on the vehicle pressure profiles, which could be extrapolated to a sonic boom signature. The Wind-US and Cart3D computational fluid dynamic (CFD) codes were used for this analysis. Three types of nozzle plumes were studied: an axisymmetric convergent-divergent nozzle, an axisymmetric plug nozzle, and a high aspect ratio nozzle. Two vehicle configurations were studied: a 59° delta wing-body model and a 69° swept wing-body model. The pressure profiles from these configurations are presented and compared to a baseline vehicle with no propulsion to demonstrate the effect of the nozzle exhaust plume.

2.0 Computational Modeling

2.1 Wind-US

Three types of exhaust nozzles were modeled with Wind-US: (1) a convergent-divergent supersonic nozzle replica of "Nozzle 6" (Ref. 5), (2) a plug nozzle, and (3) a high aspect ratio convergent-divergent supersonic slot nozzle. The configurations will be discussed in Section 3.0. Wind-US is a general purpose fluid flow solver that is used to numerically solve various sets of equations governing physical phenomena (Ref. 10). Wind-US was used to take advantage of the established capability to correctly compute nozzle plumes with viscous and turbulence effects. The code supports the solution of the Euler and Navier-Stokes equations, along with supporting equation sets governing turbulent and chemically-reacting flows. The flow solver is parallel and can take advantage of multi-core and multi-cpu hardware. The version used was Wind-US 2.0. Wind-US was used with the modified second-order Roe upwind scheme for stretched grids, implicit time stepping with a Courant–Friedrichs–Lewy (CFL) number of 1.0, and the Menter shear stress transport (SST) turbulence model.

2.2 Cart3D

Two vehicle configurations were studied using Cart3D: (1) a 59° delta wing-body model and (2) a 69° swept wing-body model. The vehicle configurations were fully three-dimensional models, and will be discussed in Section 3.0. Cart3D is a high-fidelity inviscid analysis package for conceptual and preliminary aerodynamic design. It allows users to perform automated CFD analysis on complex geometry. Geometry for Cart3D is in the form of surface triangulations. These may be generated from within a Computer-Aided Design (CAD) package, from legacy surface triangulations or from structured surface grids. Cart3D uses adaptively refined Cartesian grids to discretize the space surrounding a geometry and cuts the geometry out of the set of "cut-cells" which intersect the surface triangulation. The flow solver is parallel and can take advantage of multi-core and multi-cpu hardware. Solutions used the Cart3D adjoint adaptation module. This module uses adjoint-weighted residual error-estimates to drive mesh adaptation. Once a user specifies outputs of interest (lift, drag, etc.) with a corresponding error tolerance, this module automatically meshes the simulation to drive the remaining numerical errors in the outputs below the requested tolerance. This module has been validated for sonic boom prediction by Wintzer (Ref. 11), and this capability was the reason Cart3D was selected for analysis of this problem. The adaptation module allows greatly reduced time spent on mesh generation and analysis.

3.0 Geometry Modeling

3.1 Nozzles

For the nozzle configurations, the computational domain was an axisymmetric structured grid which consisted of 8 zones, and 511,299 grid points. The slot nozzle simulation was a similar two-dimensional structured grid. The domain extended 18 nozzle diameters downstream of the nozzle exit. Multi-block wall-packed grids were generated for use on parallel processor systems. Viscous wall boundaries were used for all nozzle surfaces. Convergence was monitored with nozzle mass flow and the off-body pressure profile at 150 in. from the nozzle centerline. External flow conditions were run at Mach 2.2 and an angle of attack of zero. Cases were run on a local computer cluster and took approximately 6 to 8 hr to converge.

3.1.1 Convergent-Divergent Nozzle

Figure 1 displays the Mach 2.0 supersonic convergent-divergent exhaust nozzle, which was a replica of the Putnam "Nozzle 6." This nozzle had a design pressure ratio of 8.12 and simulations were performed from NPR = 6 to 18. For the wing-body model propulsion-integration analysis, described in Section 3.2, the simulation was performed at an under-expanded pressure ratio of 18, where a highly under-expanded plume was selected with the intent to demonstrate a significant plume effect. If successful, a NPR closer to the design point would be studied. The CFD grid is shown in Figure 3(a) and the nozzle plume shape in Figure 4(a). The shape of the nozzle plume was extracted from the simulation and imported into grid generation software, where the nozzle plume was modeled as a solid body. Use of solid body models of nozzle plumes was validated by both Putnam (Ref. 5) and Castner (Ref. 9).

3.1.2 Plug Nozzle

The plug nozzle was simplified to a single stream nozzle, and was a replica of the Chenoweth (Ref. 12) nozzle core stream only, shown in Figure 2. The design pressure ratio was 26.3 and simulations were performed at NPR = 8, 14, and 18. Again, the wing-body simulation was performed at a NPR = 18. The CFD grid is shown in Figure 3(b) and the resulting nozzle plume shape in Figure 4(b). For the wing-body model analysis, the plume was extracted from the simulation and imported into grid generation software and the nozzle plume was modeled as a solid body.

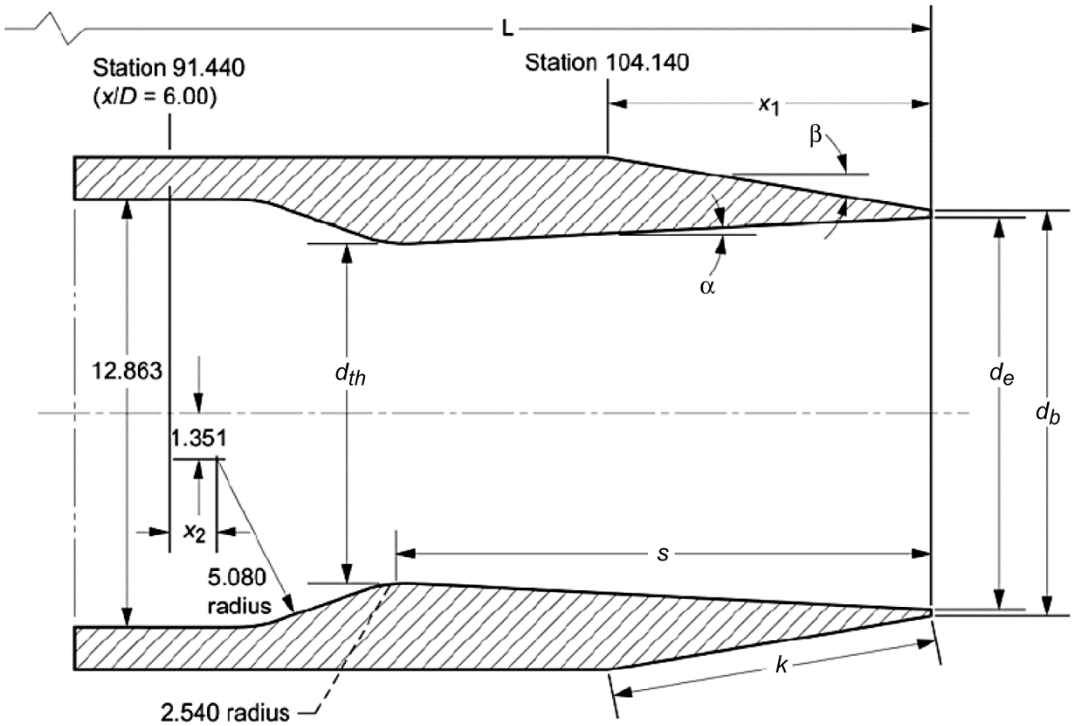

Nozzle	$M_{j,des}$	$(P_{t,j}/P_\infty)_{des}$	α, deg.	β, deg.	x_1	L	k	s	d_{th}	d_e	d_b	A_{th}	A_e	A_e/A_{th}	x_2
1	2.920	32.58	11.50	0	15.240	119.380	15.240	18.519	7.577	15.011	15.240	45.09	176.98	3.925	2.908
2	2.272	11.97	7.28	0	15.240	119.380	15.240	18.747	10.264	15.011	15.240	82.75	176.98	2.139	4.224
3	2.740	24.77	11.50	0	12.192	116.332	12.192	16.878	8.255	15.011	15.240	53.52	176.98	3.307	2.118
4	2.523	17.72	11.50	0	9.144	113.284	9.144	14.883	9.144	15.011	15.240	65.66	176.98	2.695	2.118
5	2.267	11.88	9.06	0	9.144	113.284	9.144	15.011	10.288	15.011	15.240	83.12	176.98	2.129	1.953
6	2.024	8.12	6.04	5	9.109	113.249	9.144	15.105	10.223	13.417	13.646	82.08	141.39	1.722	1.778
7	1.700	4.94	3.04	10	8.999	113.139	9.144	15.166	10.231	11.836	12.065	82.21	110.03	1.338	1.580

Figure 1.—Convergent-divergent "Nozzle 6" (Ref. 5).

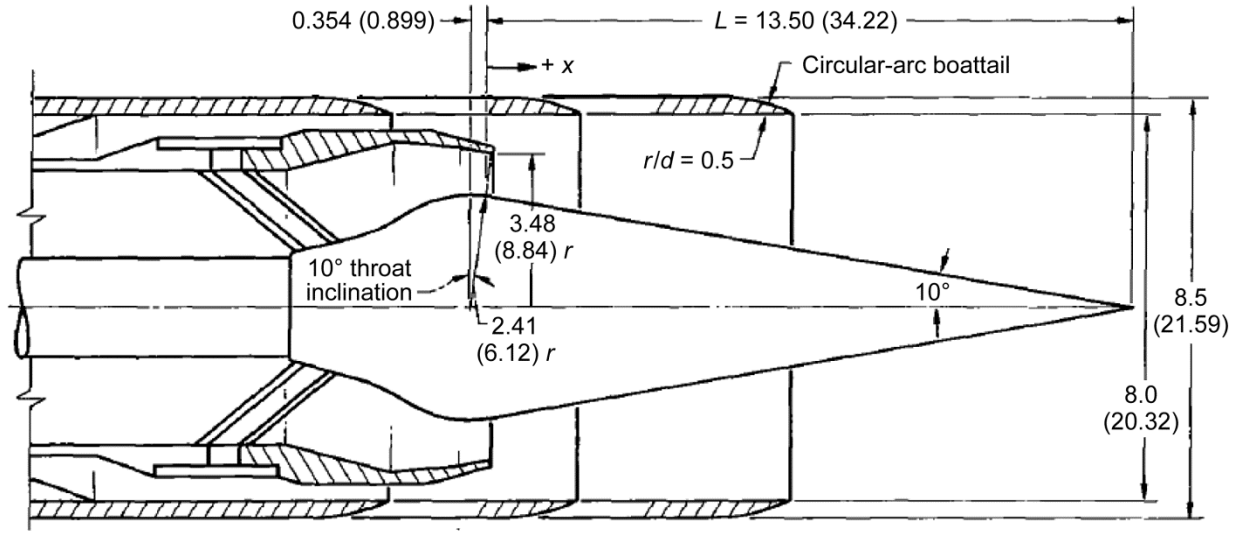

Figure 2.—Plug nozzle (Ref. 12).

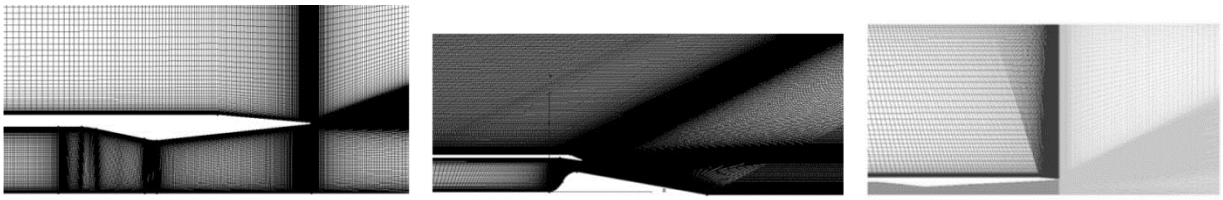

(a) (b) (c)

Figure 3.—Wind-US grid for (a) convergent-divergent nozzle, (b) plug nozzle, and (c) slot nozzle.

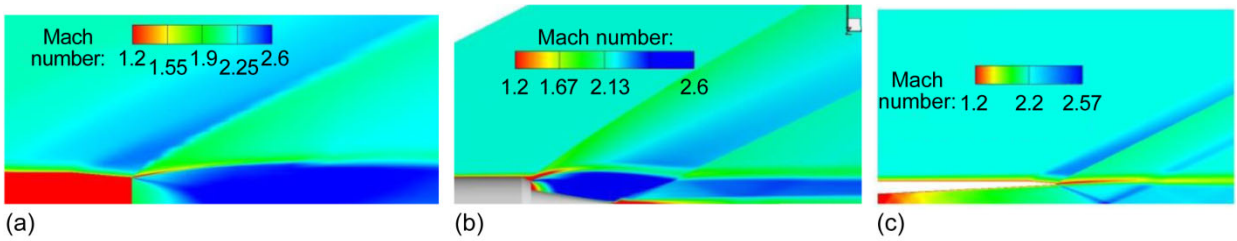

(a) (b) (c)

Figure 4.—Wind-US solutions (Mach number contour) for (a) convergent-divergent nozzle, (b) plug nozzle, and (c) slot nozzle.

3.1.3 Slot Nozzle

A fully-expanded Mach 2.2 slot nozzle was designed, operating at a NPR = 12, for highly under-expanded flow. The NPR = 12 plume was selected due to the excessive size of the plume at NPR = 18. The nozzle was a simple convergent-divergent geometry with a throat height of 2.05 in. and an exit height of 3.88 in. There was a short external boat-tail of 5°, and an external height of 4.57 in. The CFD grid is shown in Figure 3(c). In the wing-body analysis, the slot nozzle had an effect on a larger portion of the wing area, so a smaller plume shape at the reduced pressure ratio was selected. The nozzle plume shape (Fig. 4(c)) was extracted from the simulation and imported into grid generation software and the nozzle plume was modeled as a solid body. In the wing-body analysis the nozzle had an aspect ratio of 11.2:1.

3.2 Vehicles

Two vehicle configurations, from Hunton (Ref. 13), were studied (Fig. 5): a 59° delta wing-body model and a 69° swept wing-body model. Vehicles were studied with a notional 4-engine configuration. Figure 6 shows a comparison between the Concorde (Ref. 1) and the 59° delta wing-body model, with the scale factor estimated at 9:1. Table 1 shows comparisons between some key aircraft dimensions.

For the Cart3D CFD analysis, the original wing-body vehicle scale was increased by a factor of 14.11, where the vehicle body diameter was modeled as 15.1 in. This diameter allowed use of previous modeling work that was performed with the 59° delta wing-body vehicle and Putnam's "Nozzle 6". At this scale, the notional propulsion was 3.38 in. in diameter (instead of a very small 0.23 in. diameter). Dimensions of the nozzles are given in Table 2. Exit area and throat area were not held constant during this study, and the plug nozzles were nominally 24 percent larger in diameter than the convergent-divergent nozzle. A size for "Nozzle 6" was estimated from the Concorde propulsion system, assuming 10,000 lb of thrust per engine at cruise conditions, and then geometrically reduced to the nominally 1/9 scale difference between the Concorde and the model. When the same procedure was used for the plug nozzle, there was a difference in exit area.

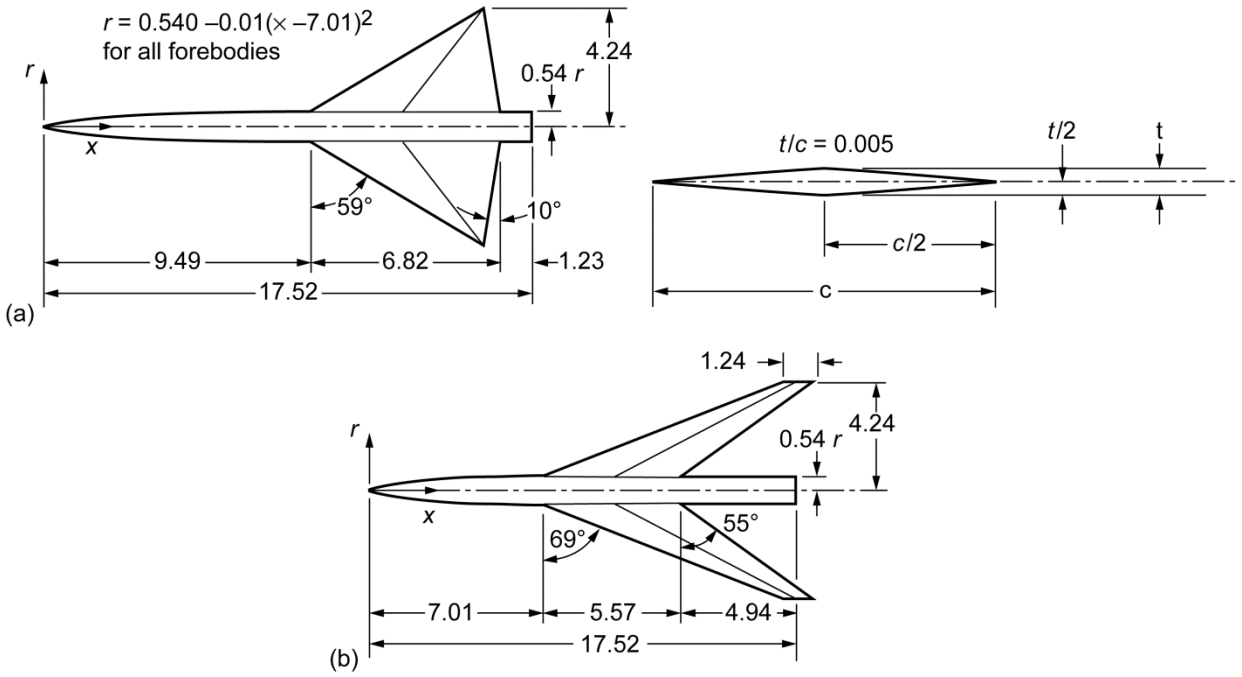

Figure 5.—Dimensions for (a) delta wing-body model and (b) swept wing-body model, before being scaled up by a factor of 14.11.

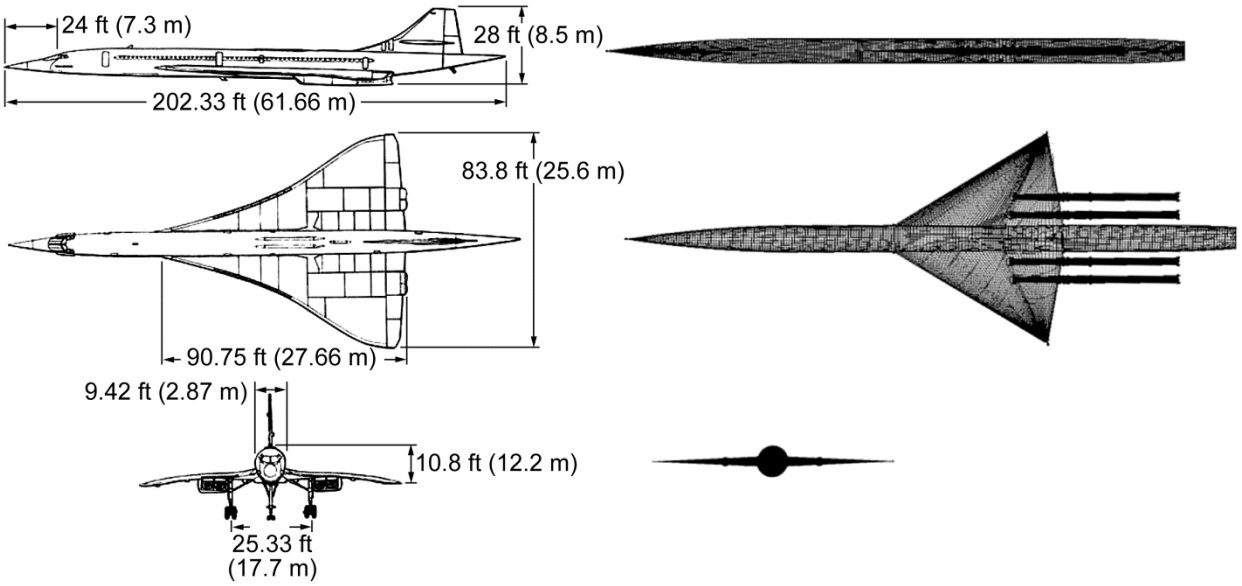

Figure 6.—Comparison of the Concorde (Ref. 1) to the delta wing-body model (scaled to a wingspan of 446 in.).

TABLE 1.—COMPARISONS BETWEEN THE CONCORDE AND THE 59° DELTA WING-BODY MODEL

Concorde		59° delta wing-body		Scale factor (Concorde: Delta wing-body dimensions)
Length	2428 in.	Length	247.5 in.	9.8 : 1
Wing Span	446 in.	Wing span	52.3 in.	8.5 : 1

TABLE 2.—KEY NOZZLE DIMENSIONS

Nozzle	NPR	T_0	Exit area sq-in.	Exit diameter, in.	Outer diameter, in.
Convergent-divergent	8, 18	530 R	2.66	3.38	3.75
Plug	8, 18	530 R	4.9	3.52	4.64
	NPR	T_0	Exit area sq-in.	Exit width, in.	Exit height, in.
Slot	12	530 R	2.8	5.6	0.5

The model was run on the Pleiades computer cluster at the NASA Ames Research Center. The adjoint adaptation module uses Open MultiProcessing (OpenMP) for code parallelization within a node, and at the time of writing, could not utilize message passing interface (MPI) to work between nodes, required on Peliades architecture. As a result, a single node with 12 processors was used until the node ran out of memory, at approximately 4.5 million cells.

3.2.4 59° Delta Wing-Body Model

The 59° delta wing-body model was a simplified platform for a propulsion integration study on sonic boom. The wing-body model was modified with a long sting, tapered at the trailing end. The tapered sting was installed to eliminate the effects of a tail cone and tail, so propulsion effects could be studied with a focus on the nozzle plume. The overall length of the body and sting was 398.9 in., and the trailing portion of the sting had the same geometry as the nosecone. Engines were installed in an embedded configuration at the back of the wing as shown in Figure 7. Embedded nozzles were used to isolate plume effects, without the effects of an inlet flow field. The engine plumes were constructed of the actual exhaust plume shape, followed by a cylindrical solid body (rectangular solid body for the slot nozzle). The cylindrical portion was extended aft to a point where the termination of the plume would not affect the pressure signature from the nose, wing, and nozzles. The configurations tested with the 59° delta wing-body model are shown in Table 3, and included three different levels of engine placement (spacing and stagger).

3.2.5 69° Swept Wing-Body Model

The 69° swept wing-body model was used as an alternate platform for propulsion integration studies. The swept wing-body model was also modified with a long sting, tapered at the trailing end, so propulsion effects could be studied with a focus on the nozzle plume. Engines were installed at the back of the wing as shown in Figure 8. Again, embedded nozzles were used to isolate plume effects. For this configuration the engine locations were studied at three positions, locations are shown in Figure 9. The engine plumes were again constructed of the actual exhaust plume shape, followed by a cylindrical solid body. The cylindrical portion was extended aft to a point where the termination of the plume would not affect the pressure signature from the nose, wing, and nozzles. The configurations tested with the 69° swept wing-body model are also shown in Table 3.

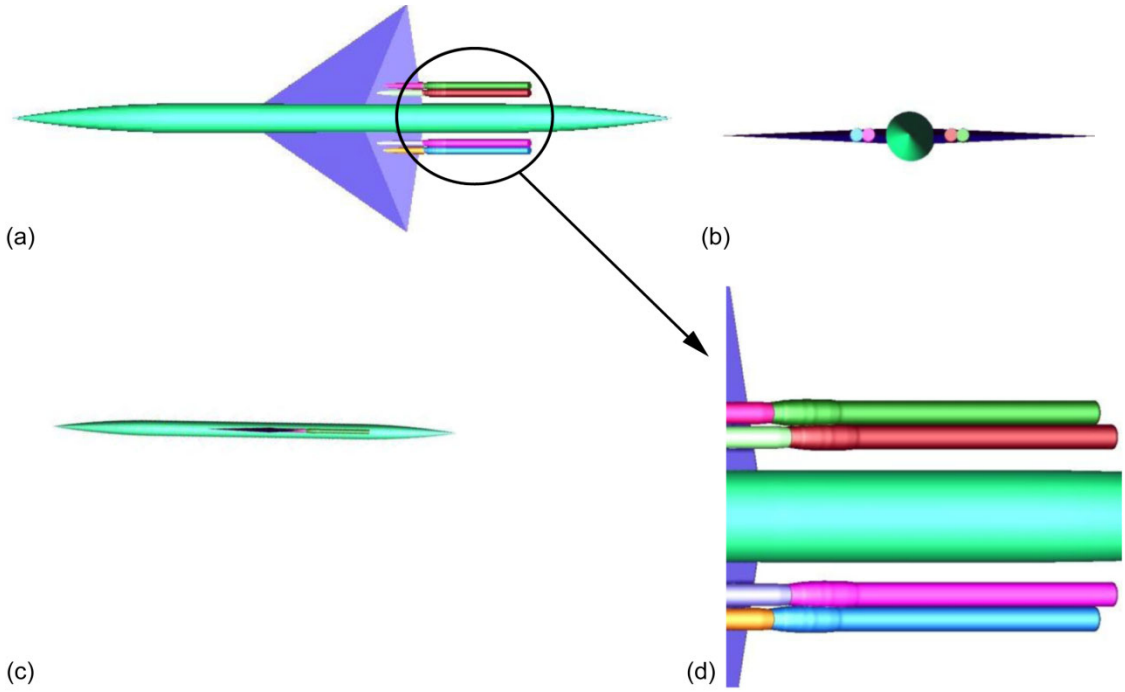

Figure 7.—Cart3D model of the delta wing-body model with convergent-divergent nozzles installed (a) top view, (b) back view, (c) left side view, and (d) plume shape.

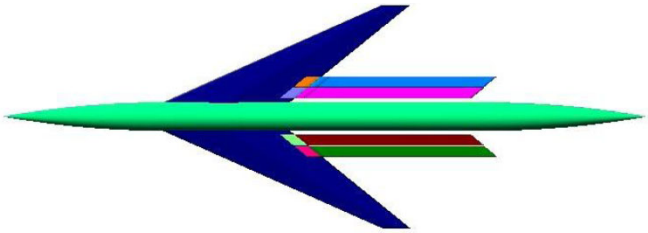

Figure 8.—Cart3D model of the swept wing-body model with slot nozzles installed, top view.

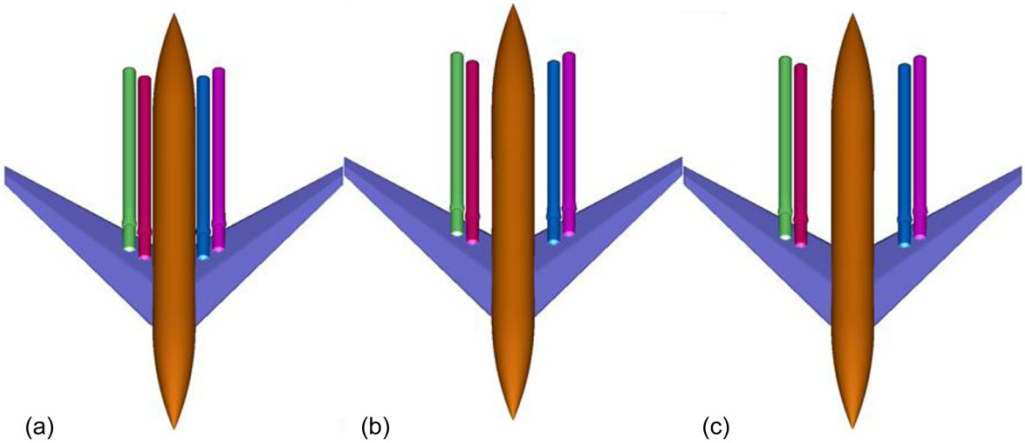

Figure 9.—Cart3D model of the swept wing-body model with convergent-divergent nozzles installed, (a) inner, (b) middle, and (c) outer engine mounting positions.

TABLE 3.—59° DELTA WING-BODY MODEL AND 69° SWEPT WING-BODY MODEL CONFIGURATIONS

Configuration	Vehicle type	Nozzle type	Inboard nozzle location, in.	Nozzle spacing, nozzle diameters	Nozzle stagger, nozzle diameters	NPR	Mach / T_{∞},R
C430	Delta-wing	C-D	13.17	3	0	18	2.2 / 530
C413	Delta-wing	C-D	13.17	1	3	18	2.2 / 530
C410	Delta-wing	C-D	13.17	1	0	18	2.2 / 530
P430	Delta-wing	Plug	13.17	3	0	18	2.2 / 530
P413	Delta-wing	Plug	13.17	1	3	18	2.2 / 530
S451	Delta-wing	Slot	12.64	1	0	12	2.2 / 530
C411i	Swept-wing	C-D	9.5	1	1	8, 18	2.2 / 530
C411m	Swept-wing	C-D	13.5	1	1	8, 18	2.2 / 530
C411o	Swept-wing	C-D	17.5	1	1	8, 18	2.2 / 530
P411i	Swept-wing	Plug	9.9	1	1	8, 18	2.2 / 530
P411m	Swept-wing	Plug	13.9	1	1	8, 18	2.2 / 530
P411o	Swept-wing	Plug	17.9	1	1	8, 18	2.2 / 530
S451	Swept-wing	Slot	12.64	1	0	12	2.2 / 530

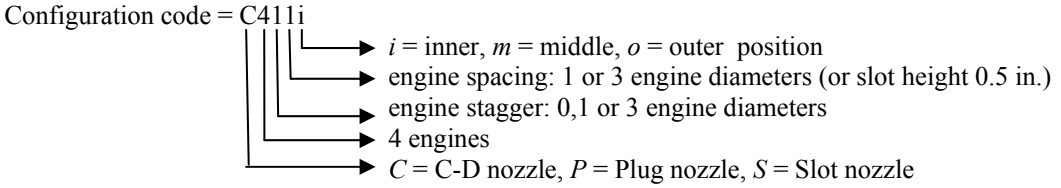

4.0 Results

Pressure profiles ($\Delta P/P$) were computed at three body lengths ($h = 3\ L_v$) below the vehicle. Three sets of results will be presented: (1) pressure profiles for the 59° delta wing-body model at a NPR = 18, (2) pressure profiles for the 69° swept wing-body model at a NPR = 18, and (3) pressure profiles for the 69° swept wing-body model at a NPR = 8. Propulsion was analyzed with different levels of engine placement, including spacing and stagger (i.e., one nozzle exit plane located behind the other).

4.1 $\Delta P/P$ Pressure Profile for 59° Delta Wing-Body Model

Pressure profiles are displayed in Figure 10 for the 59° delta wing-body model at a distance of three vehicle lengths ($h = 3\ L_v$) below the vehicle. Major features in these pressure profiles include the nose shock, wing shock, wing expansion, and trailing shock back to ambient pressure. The baseline vehicle pressure signature is the 59° delta wing-body model with no propulsion installed. Configurations with propulsion installed all had a small reduction in the peak-to-peak magnitude of the pressure profile. It was difficult to differentiate been the pressure profiles for most nozzle installations. Only two configurations demonstrated a small improvement over the others: (a) the slot nozzle configuration and (b) the plug nozzle with a spacing of 3 and no stagger. These results did not demonstrate a significant impact on the overall peak-to-peak magnitude of the pressure profile, and were only useful for a small improvement in the vehicle pressure profile.

4.2 $\Delta P/P$ Pressure Profile for 69° Swept Wing-Body Model, NPR = 18

Figure 11 shows the pressure profiles at a location three vehicle lengths below the vehicle for the swept wing-body model with convergent-divergent (C-D) nozzles operating at a NPR = 18. In this case, the pressure profile is characterized by a nose shock, a wing shock, the nozzle lip shock, and the trailing shock. For the C-D nozzles, all configurations showed a favorable reduction in the peak-to-peak value of the pressure profile, when compared to the baseline vehicle with no propulsion. As the engine nacelles were moved from their inboard, to middle, to outboard location along the wing-span, there was a reduction in the magnitude of the trailing shock, which would be favorable for a reduction in sonic boom.

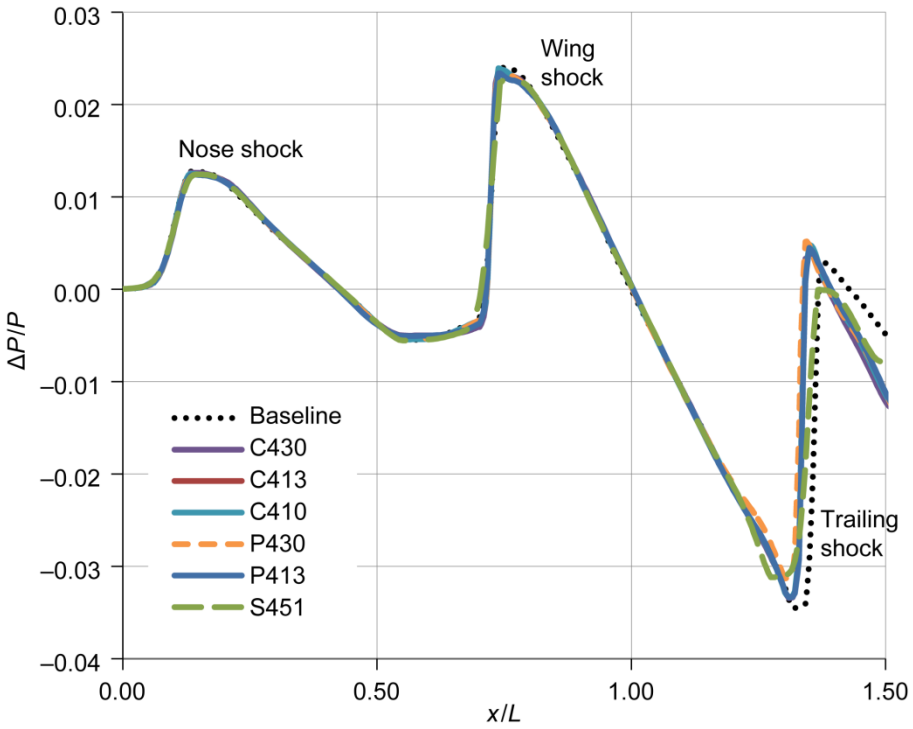

Figure 10.—Delta wing-body pressure profiles ($\Delta P/P$) at h = 3 L_V below vehicle.

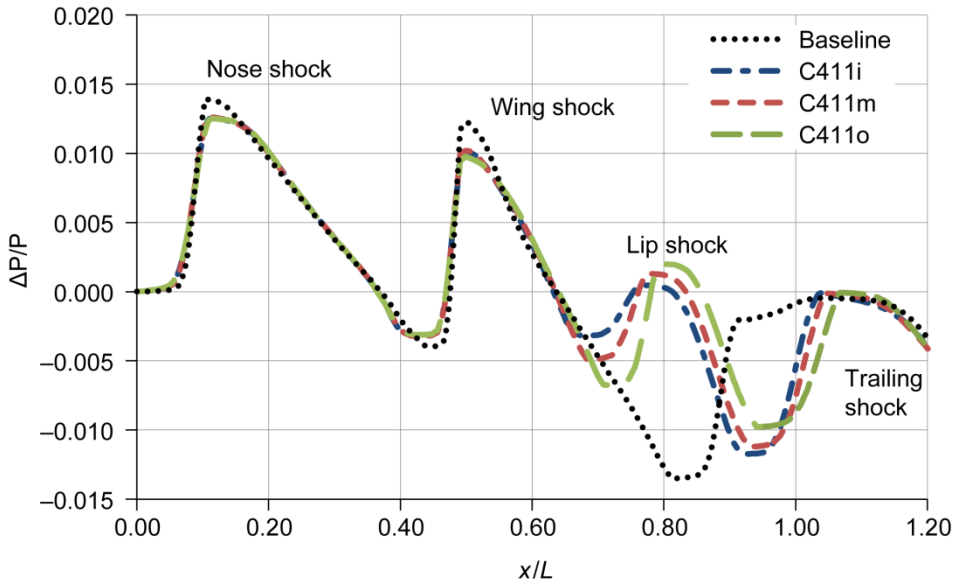

Figure 11.—Swept wing-body pressure profiles ($\Delta P/P$) for convergent-divergent nozzle configurations, NPR = 18, h = 3 L_V below vehicle.

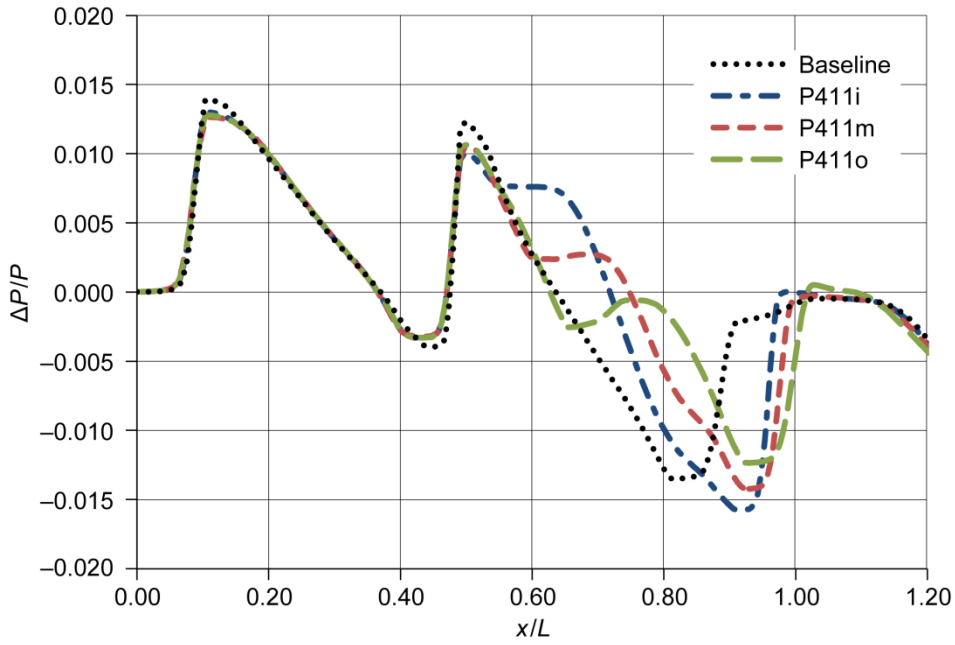

Figure 12.—Swept wing-body pressure profiles ($\Delta P/P$) for plug nozzle configurations, NPR = 18, h = 3 L_V below vehicle.

Figure 12 shows the pressure profiles for the swept wing-body model with plug nozzles operating at NPR = 18, also at three vehicle lengths below the vehicle. When compared to the baseline vehicle with no propulsion, the peak-to-peak pressure profile was increased with the addition of plug nozzles located at the inboard location along the wing-span. As the engines were moved to the middle and outboard locations, the magnitude of the trailing shock decreased. For this study, the plug nozzles were 25 percent larger than the C-D nozzles and were potentially too large to have a beneficial effect on the pressure profile. This type of detrimental effect on sonic boom was previously demonstrated in studies of isolated nozzles where an underexpanded plume reduced the near-field pressure profile for moderate increases in NPR, but a large increase in NPR caused an increase in the peak-to-peak pressure profile (Ref. 6). Results for the slot nozzle case are not shown as it had no improvement over the C-D or the plug nozzle results.

4.3 $\Delta P/P$ Pressure Profile for 69° Swept Wing-Body Model, NPR = 8

Simulations from the previous section resulted in under-expanded nozzle flow. For the C-D nozzle, the design point was a NPR = 8. At this point, the thrust coefficient was computed to be 0.99, but at NPR = 18 the thrust coefficient was reduced to 0.91. To study the effect at the design point, simulations for the swept wing-body geometry were re-calculated using a NPR = 8.

Figure 13 contains the pressure profiles for the C-D nozzles at NPR = 8. All configurations showed a favorable reduction in the peak-to-peak value of the pressure profile, when compared to the baseline vehicle with no propulsion. Again, as the engine nacelles were moved from their inboard, to middle, to outboard location along the wing-span, there was a reduction in the magnitude of the trailing shock. For the C-D nozzles operating at their design point, these profiles show the benefit that this embedded prolusion configuration has on a generic swept wing vehicle.

Figure 14, shows results for the plug nozzles at NPR = 8 (on the swept wing-body vehicle). As before, when compared to the baseline vehicle with no propulsion, the peak-to-peak pressure profile was increased with the addition of plug nozzles located at the inboard location along the wing-span. As the engines were moved to the middle and outboard locations, the magnitude of the trailing shock again was

decreased. These results suggest that the underexpanded plume shape generated by the plug nozzle at NPR = 18 was too large to be of benefit for this configuration, but operation at NPR = 8 showed reductions in the peak-to-peak value of the pressure profile as the engine locations were moved outward. This is again similar to the effect found in isolated nozzle research, where an underexpanded plume reduced the near-field pressure profile for moderate increases in NPR, but a large increase in NPR caused an increase in the peak-to-peak pressure profile.

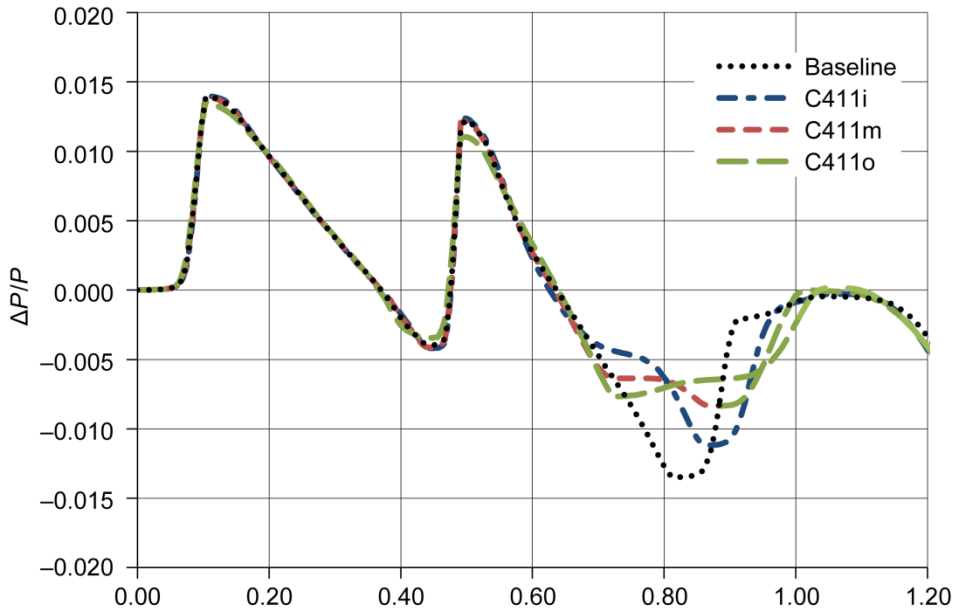

Figure 13.—Swept wing-body pressure profiles ($\Delta P/P$) for convergent-divergent nozzle configurations, NPR = 8, h = 3 L_V below vehicle.

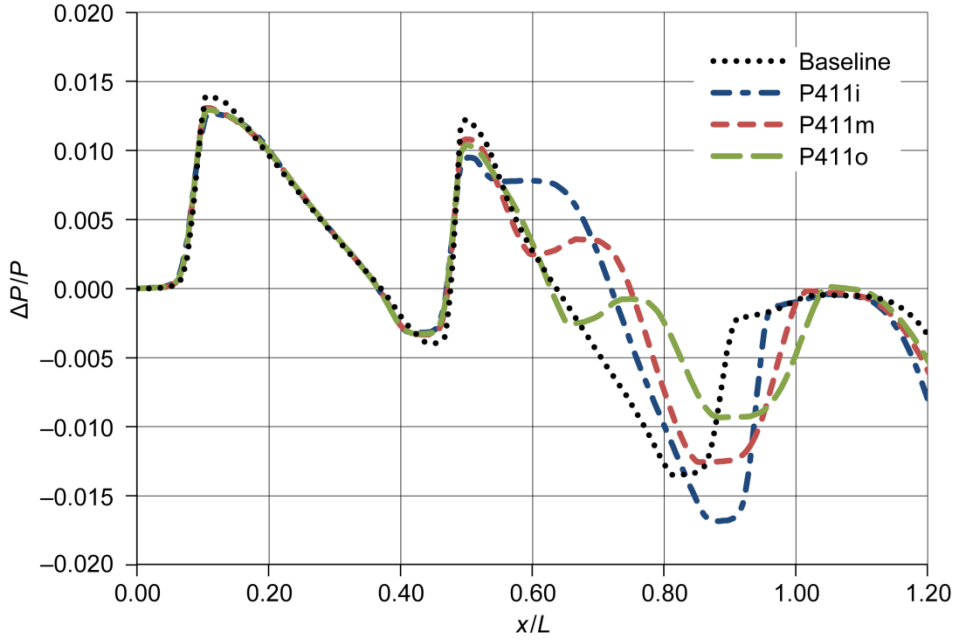

Figure 14.—Swept wing-body pressure profiles ($\Delta P/P$) for plug nozzle configurations, NPR = 8, h = 3 L_V below vehicle.

5.0 Conclusions

Three types of nozzles and two types of wing-body vehicles were used to study propulsion integration for nozzle plume effects on sonic boom. The study was not intended to be an aircraft design, but an attempt to isolate nozzle plume effects on a simple integrated configuration. The vehicle configuration did not include a tail cone, vertical tail, or horizontal stabilizer.

Results for the delta wing-body vehicle indicated that the three different types of nozzles had a small effect on the overall pressure profile, showing only 10 percent improvement in the trailing shock strength. The shock and expansion wave from the delta wing was stronger than the shock and expansion from the swept wing, and the nozzle lip shock was not able to affect the wing expansion as seen in past studies of isolated nozzles.

Changes in the pressure profile were favorable for the swept wing-body configuration, where convergent-divergent nozzles produced a reduction in the trailing shock. The plug nozzles, when operating at NPR = 8, also produced a reduction in the trailing shock. The exhaust plumes reduced the peak-to-peak magnitude of the pressure profile as the nozzles were moved outward along the wing-span. Movement of the nozzles resulted in a 28 to a 44 percent reduction in the strength of the trailing shock, depending on nozzle pressure ratio.

This preliminary study utilized a stepping stone approach to focus on how nozzle plumes interact with the wing-body vehicle. Nozzle plume effects for a four engine vehicle have a visible effect on the near field pressure profile. Based on the improvements in near field profiles, the following future analysis are feasible: (1) a design of experiments study to determine optimum nozzle placement and pressure ratio, and (2) a study which includes the addition of the vehicle tail-cone and tail.

References

1. "Concorde SST: History," Concorde SST, http://www.concordesst.com/history/historyindex.html [retrieved 24 February 2011].
2. "Supersonic Aircraft Noise," http://www.faa.gov/about/office_org/headquarters_offices/ apl/noise_emissions/ supersonic_aircraft_noise/ [retrieved 5 December 2011].
3. Freund, D., Howe, D., Simmons, F., and Schuester, L., "Quiet Spike Prototype Aerodynamic Characteristics From Flight Test," AIAA−2008−125, Jan. 2005.
4. Graham, D., Dahlin, J., Meredith, K., and Vadnais, J., "Aerodynamic Design of Shaped Sonic Boom Demonstration Aircraft," AIAA−2005−8, Jan. 2005.
5. Putnam, L. and Capone, F., "Experimental Determination of Equivalent Solid Bodies to Represent Jets Exhausting into a Mach 2.20 External Stream," NASA TN-D-5553, 1969.
6. Castner, R.S., "Analysis of Plume Effects on Sonic Boom Signature for Isolated Nozzle Configurations," NASA/TM—2008-215414 (AIAA−2008−3729), June 2008.
7. Bui, T., "CFD Analysis of the Nozzle Jet Plume Effects on Sonic Boom Signature," AIAA−2009−1054, Jan. 2009.
8. Castner, R.S., "Slot Nozzle Effects for Reduced Sonic Boom on a Generic Supersonic Wing Section," AIAA−2010−1386, Jan. 2010.
9. Castner, R.S., "Analysis of Exhaust Plume Effects on Sonic Boom for a 59-Degree Wing Body Model," AIAA−2011−917, Jan. 2011.
10. Towne, C.E., "Wind-US Users Guide, Version 2.0," NASA/TM—2009-215804, Oct. 2009.
11. Wintzer, M., Nemec, M., and Aftosmis, M., "Adjoint-Based Adaptive Mesh Refinement for Sonic Boom Prediction," AIAA−2008−6593, Aug. 2008.
12. Chenoweth, F.C., and Lieberman, A., "Experimental Investigation of Heat-Transfer Characteristics of a Film-Cooled Plug Nozzle With Translating Shroud," NASA TN D-6160, Feb. 1971.
13. Hunton, L., Hicks, R., and Mendoza, J., "Some Effects of Wing Planform on Sonic Boom," NASA TN-D 7160, Jan. 1973.

REPORT DOCUMENTATION PAGE	Form Approved OMB No. 0704-0188

1. REPORT DATE *(DD-MM-YYYY)*	2. REPORT TYPE	3. DATES COVERED *(From - To)*
01-04-2012	Technical Memorandum	

4. TITLE AND SUBTITLE
Exhaust Plume Effects on Sonic Boom for a Delta Wing and a Swept Wing-Body Model

5a. CONTRACT NUMBER

5b. GRANT NUMBER

5c. PROGRAM ELEMENT NUMBER

6. AUTHOR(S)
Castner, Raymond; Lake, Troy

5d. PROJECT NUMBER

5e. TASK NUMBER

5f. WORK UNIT NUMBER
WBS 984754.02.07.03.13.02

7. PERFORMING ORGANIZATION NAME(S) AND ADDRESS(ES)
National Aeronautics and Space Administration
John H. Glenn Research Center at Lewis Field
Cleveland, Ohio 44135-3191

8. PERFORMING ORGANIZATION REPORT NUMBER
E-18176

9. SPONSORING/MONITORING AGENCY NAME(S) AND ADDRESS(ES)
National Aeronautics and Space Administration
Washington, DC 20546-0001

10. SPONSORING/MONITOR'S ACRONYM(S)
NASA

11. SPONSORING/MONITORING REPORT NUMBER
NASA/TM-2012-217446

12. DISTRIBUTION/AVAILABILITY STATEMENT
Unclassified-Unlimited
Subject Categories: 02 and 07
Available electronically at http://www.sti.nasa.gov
This publication is available from the NASA Center for AeroSpace Information, 443-757-5802

13. SUPPLEMENTARY NOTES

14. ABSTRACT
Supersonic travel is not allowed over populated areas due to the disturbance caused by the sonic boom. Research has been performed on sonic boom reduction and has included the contribution of the exhaust nozzle plume. Plume effect on sonic boom has progressed from the study of isolated nozzles to a study with four exhaust plumes integrated with a wing-body vehicle. This report provides a baseline analysis of the generic wing-body vehicle to demonstrate the effect of the nozzle exhaust on the near-field pressure profile. Reductions occurred in the peak-to-peak magnitude of the pressure profile for a swept wing-body vehicle. The exhaust plumes also had a favorable effect as the nozzles were moved outward along the wing-span.

15. SUBJECT TERMS
Sonic booms; Exhaust nozzle; Computational fluid dynamic (CFD); Exhaust gases; Plumes; Delta wings; Body-wing configurations

16. SECURITY CLASSIFICATION OF:			17. LIMITATION OF ABSTRACT	18. NUMBER OF PAGES	19a. NAME OF RESPONSIBLE PERSON
a. REPORT	b. ABSTRACT	c. THIS PAGE			STI Help Desk (email:help@sti.nasa.gov)
U	U	U	UU	19	19b. TELEPHONE NUMBER *(include area code)* 443-757-5802